Journal of Nuclear Science and Technology

ISSN: 0022-3131 (Print) 1881-1248 (Online) Journal homepage: https://www.tandfonline.com/loi/tnst20

Extensive Study of the Soft-Rotator Model Hamiltonian Parameters for Medium and Heavy Even-Even Nuclei

Satoshi KUNIEDA , Satoshi CHIBA , Keiichi SHIBATA , Akira ICHIHARA , Osamu IWAMOTO , Nobuyuki IWAMOTO , Tokio FUKAHORI & Efrem Sh. SUKHOVITSKIĬ

To cite this article: Satoshi KUNIEDA , Satoshi CHIBA , Keiichi SHIBATA , Akira ICHIHARA , Osamu IWAMOTO , Nobuyuki IWAMOTO , Tokio FUKAHORI & Efrem Sh. SUKHOVITSKIĬ (2009) Extensive Study of the Soft-Rotator Model Hamiltonian Parameters for Medium and Heavy Even-Even Nuclei, Journal of Nuclear Science and Technology, 46:9, 914-924, DOI: 10.1080/18811248.2009.9711600

To link to this article: https://doi.org/10.1080/18811248.2009.9711600

Published online: 16 Mar 2012.

Journal of NUCLEAR SCIENCE and TECHNOLOGY, Vol. 46, No. 9, p. 914–924 (2009)

ARTICLE

Extensive Study of the Soft-Rotator Model Hamiltonian Parameters for Medium and Heavy Even-Even Nuclei

Satoshi KUNIEDA[1,*], Satoshi CHIBA[1,2], Keiichi SHIBATA[1], Akira ICHIHARA[1], Osamu IWAMOTO[1], Nobuyuki IWAMOTO[1], Tokio FUKAHORI[1] and Efrem Sh. SUKHOVITSKIĬ[3]

[1]*Japan Atomic Energy Agency, Tokai-mura, Naka-gun, Ibaraki-ken 319-1195, Japan*
[2]*National Astronomical Observatory of Japan, 2-21-1 Osawa, Mitaka, Tokyo 181-8588, Japan*
[3]*Joint Institute for Energy and Nuclear Research, 220109 Minsk-Sosny, Belarus*

(Received October 30, 2008 and accepted in revised form May 18, 2009)

Soft-rotator model Hamiltonian parameters were deduced for 63 even-even nuclei in the mass range $56 \leq A \leq 238$ by a combination of low-lying level structure and coupled-channel proton scattering analyses toward a systematic and accurate calculation of nuclear data. It was found that the obtained effective quadrupole and octupole deformation parameters were consistent with those derived from experimental $B(E2)$ and $B(E3)$ data. In addition, equilibrium ground-state quadrupole deformation parameters were also in reasonable accord with theoretical results for deformed heavy nuclei. The obtained parameters often varied with neutron and/or proton numbers anomalously, showing mostly the effects of shell closure. On the other hand, some clear systematic trends were seen among major Hamiltonian parameters.

KEYWORDS: soft-rotator model, coupled-channel optical model, collective nature, Hamiltonian parameters, even-even nuclei, medium and heavy nuclei, level structure, inelastic proton scattering cross sections, anomalous behaviors, systematic trends

I. Introduction

Nuclear collective excitation is one of the important phenomena in which a nucleus shows its own coherent properties. It affects the nucleon-induced cross sections in low to medium energy regions significantly. Recently, the soft-rotator model[1,2] (SRM) analysis has successfully enabled the description of the low-lying levels and collective natures of some even-even nuclei. At the same time, the coupled-channel (CC) optical model analysis has also been carried out using the nuclear properties described by the SRM (SRM-CC), which resulted in successful nucleon-nucleus interaction studies. For instance, it has been reported by Chiba and coworkers for ^{12}C,[1,3] by Sukhovitskiĭ and coworkers for ^{58}Ni,[4] ^{56}Fe,[5] and ^{52}Cr,[6] and by Sun *et al.* for ^{28,30}Si.[7] In the model, each nucleus is assumed to have its own shape in the ground and excited states, and collective excitations are ascribed to the rotational-vibrational motion. It is the substantial feature of the SRM that such concepts are considered for the quadrupole, octupole, and hexadecapole modes. The model is expected to be applicable to the analyses of various rotational-vibrational even-even nuclei.

The main purpose of this study is to deduce SRM Hamiltonian parameters systematically for a number of even-even nuclei. The present work is devoted only to the study of the Hamiltonian, while the past ones also put emphasis on a consistent SRM-CC cross section analysis for neutrons and protons. The analysis procedure basically follows that of the previous (original) studies referred in the preceding paragraph. Such parameters as the axial and non-axial equilibrium ground-state (G.S.) deformations, and the softness of surface vibrations are determined by a combination of SRM level structure and SRM-CC proton scattering analyses. In this work,[a] we carry out such analyses for medium and heavy nuclides for which experimental data are available for both collective-excitation levels and inelastic proton scattering cross sections, *i.e.*, 63 even-even nuclei, such as ^{56,58}Fe, ^{60,62,64}Ni, $^{64-70}$Zn, $^{70-76}$Ge, $^{74-82}$Se, ^{86}Sr, ^{96,98,100}Mo, ^{102}Ru, $^{104-110}$Pd, $^{106-116}$Cd, $^{116-124}$Sn, $^{122-130}$Te, ^{144,150}Nd, $^{148-154}$Sm, ^{160}Gd, ^{164}Dy, ^{166,168}Er, ^{174,176}Yb, ^{178,180}Hf, ^{182,184}W, ^{192}Os, ^{194}Pt, ^{232}Th, and ^{238}U. The deduced values of the deformation parameters are compared with experimental data and major theoretical mass-model results in order to investigate the validity of our results. This study is also conducted to point out/discuss some notable global trends and isotopic differences, and to investigate systematic trends of major Hamiltonian parameters.

This paper is organized as follows. We present our general approaches to SRM Hamiltonian parameter search in Sec. II. The obtained parameters are compared with experimental and theoretical mass-model predictions in Sec. III. Section III

*Corresponding author, E-mail: kunieda.satoshi@jaea.go.jp

[a] This work partially reported in Ref. 8).

is also devoted to discussions of their isotopic differences, notable behaviors, and systematic trends. Finally, Sec. IV shows our conclusions drawn from this study.

Details of the model, notations of the parameters, the search procedure, the employed database and a complete list of the deduced SRM Hamiltonian parameters will be described in a forthcoming report.[9)]

II. Parameter Search

1. Level Structure Analysis

The SRM was adopted in order to express the general feature of low-lying collective states. The model originated from the Davydov-Chaban model,[10)] which was formulated to describe the quadrupole rotational-vibrational collective motion of nonaxially deformed nuclei. The same concept was applied by Porodzinskiĭ and Sukhovitskiĭ to the octupole and hexadecapole properties.[11,12)] The model and those concepts had been integrated into one, *i.e.*, SRM, aiming at giving a general description of the low-lying collective level structure of even-even nuclei. The detailed expressions of the model are given elsewhere.[1,2)]

The SRM Hamiltonian parameters were derived from the experimentally known level data obtained by phenomenological analyses for each nucleus. Namely, we determined these parameters so as to give a good description of the measured excitation energies, spins, and parities, and band structures of low-lying levels by model calculation. The major quantities to be obtained in this analysis are the quadrupole softness $\mu_{\beta_{20}}$, the octupole softness μ_ϵ, and the quadrupole equilibrium nonaxiality γ_0. Note that the equilibrium deformation parameters $\beta_{20,(30),4}$ are estimated by SRM plus coupled-channel analysis as detailed in the next section, since they appear only as a perturbation in the level energy calculation. The parameters obtained enable us to construct an SRM wave function necessary for the cross section calculation at the later stage. The SHEMMAN code[2)] allows us to carry out model computations. In this analysis, it was essential for us to know the band structure in advance, including the G.S., nonaxial (γ-), quadrupole-vibrational (β_2-), and octupole negative-parity (β_3-) bands. It is not difficult to identify such major bands for typical deformed heavy nuclei because their low-lying collective properties are clearly characterized by rotation accompanied by vibration (so-called rotational bands). Actually, their band structures have been measured/evaluated over the ages and are well known as compiled in the series of Nuclear Data Sheets.[b] For transitional and typical vibrational nuclei, however, the band structure has not been identified in many cases. This is just because their collective natures involve a complex of various types of vibrations and rotations. Thus, for such nuclei, we were enforced to empirically assign each low-lying level to one of the members of a "plausible" band, though the values of level energy, spin, and parity were taken from the latest version of Nuclear Data Sheets. Thus, we consider that this procedure brings ambiguity to the analyses and the results to be obtained. However, we would like to emphasize that the final judgments of the band identifications were performed after confirming the best combination of the assumed level structure, the SRM parameter set, and the calculated levels that gave the least-squares deviation. Also, in order to reduce such uncertainties and carry out analyses systematically, we just considered the primary bands, *i.e.*, the G.S. band with $(\tau = 1, n_\gamma = 0, n_{\beta_2} = 0, n_{\beta_3} = 0)$, the γ-band with $(\tau = 2, n_\gamma = 0, n_{\beta_2} = 0, n_{\beta_3} = 0)$, the β_2-band with $(\tau = 1, n_\gamma = 0, n_{\beta_2} = 1, n_{\beta_3} = 0)$, and the β_3-band with $(\tau = 1, n_\gamma = 0, n_{\beta_2} = 0, n_{\beta_3} = 0)$, where the quantities in the parentheses denote quantum numbers in the SRM.

Unfortunately, it was difficult to carry out the level structure analysis of some nuclei. It was just because most of these isotopes exhibited a level structure that cannot be attributable to typical rotational-vibrational excitations. In general, the level energy ratio $E(4_1^+)/E(2_1^+)$ is almost equal to 2.0 for typical vibrational nuclei, and the value varies from $\sim$2.0 to $\sim$3.3 for rotational-vibrational nuclei. However, for example, major Zr even-even isotopes are influenced by a closed neutron shell, and their $E(4_1^+)/E(2_1^+)$ values result in $\sim$1.5. This phenomenon is beyond the SRM rotational-vibrational theory; thus, it is impossible to reproduce such level allocations using the present version of the SRM. According to these facts, we did not carry out the SRM analysis of the nuclei that apparently exhibit $E(4_1^+)/E(2_1^+) \lesssim 2.0$ even if the measured proton scattering data were abundant.

There existed another problem in the assumption of the level structure. It was difficult to identify the members of the second γ-vibrational band $(\tau = 2, n_\gamma = 1, n_{\beta_2} = 0, n_{\beta_3} = 0)$ for most of the nuclei. Actually, the band head positions in a relatively high excitation energy region where we found many candidate levels. Thus, we did not consider this band purposely in the level structure analysis. Since the level data of this band were essential for deducing the softness parameter of γ-vibration, its value was not obtained for all nuclei in this work. Note that it gives no effect on the determination of the other parameter values.

2. Coupled-Channel Optical Model Analysis

(1) Purpose of the Model Analysis

It is important to obtain a reliable value of the equilibrium G.S. deformation parameter in order to determine the whole parameter set. However, it was impossible to deduce certain values of β_{20} and β_4 just by SRM level structure analysis, since these equilibrium deformation parameters appear only as a perturbation in the level energy calculation. Thus, we tried to derive the values from the experimental data of particle inelastic scattering cross sections by optical model analysis. We employed the coupled-channel (CC) method that adopted the coupling strengths calculated using the SRM Hamiltonian. The method is called "SRM-CC" thereafter in this paper. The value of β_{20} was determined so as to describe the measured inelastic scattering data of the first 2_1^+ excitation. Also, the first 2_1^+ and 4_1^+ data were simultaneously analyzed in order to obtain the values of β_{20} and β_4 when the hexadecapole deformation was additionally assumed. Since one of the SRM parameters ϵ_0 $(= \beta_{30}/\beta_{20})$ was somewhat sensitive to the level calculations, it was

[b] Their references are listed in the recent issue.

deduced by SRM level structure analysis, while the measured cross sections were analyzed to estimate of its initial value. The CC optical model code OPTMAN[2] was adopted for such computations. The code partially includes the main part of the SHEMMAN code and enables us to carry out the SRM-CC calculations.

In this work, we restricted our efforts to the analyses of proton inelastic scattering cross sections because they are normally more abundant and accurate than neutron inelastic data. Note that this approach could be applied only to the nuclei of which inelastic proton scattering data were available. That is the reason why we carried out SRM and SRM-CC analyses for 63 nuclei mentioned previously. When experimental cross sections were available at more than two incident energies, the values of β_{20} and β_4 were determined to give an overall description of the obtained data.

(2) Optical Model Potential

The optical potential is required for SRM-CC computation. We should give an appropriate potential because it also determines the cross sections to be calculated, thereby, the deformation parameters to be estimated. It might be a natural approach for us to adjust the optical potential parameters together with the deformation parameters for each nucleus. However, the optical potential varies with the target nucleus and the projectile in general. Also, it strongly depends on the collision energy especially below 100 MeV. Furthermore, the optical potential is described with various parameters, such as potential radius, surface diffuseness, and energy-dependent potential depth parameters including the real, imaginary, volume, surface, and spin-orbit terms. A reliable parameter set should be derived not only from the measured data of the particle scattering cross section but also from the total-reaction cross section and the analyzing power.

It was expected to be a preferable approach to adopting a global optical potential of protons that covers wide nuclear mass and energy ranges. Although many global potentials have been proposed for nucleons until now, most of them could be applied in narrow nuclear-mass and energy regions. Moreover, they assume a spherical nuclear shape, as determined by single-channel calculation, while the nucleus usually exhibits collective nature where the CC method should give more successful results. For these reasons, we employed a CC optical model potential formulated by us,[13] which was derived by systematic analysis based on the rigid-rotator model (RRM-CC). The use of the RRM-CC potential in the SRM-CC calculation is reasonable and does not have a significant impact on the current study since we carried out the proton scattering analysis at comparably high energies ($\gtrsim$10 MeV) where the collective contributions progressively weaken. In this sense, the use of the spherical potential might also be acceptable. However, we adopted the CC potential in order to obtain more realistic results at around several tens of MeV for the typical deformed nuclei as well as for the other nuclei. For a complete analysis in terms of SRM-CC, however, we admit that we have to search for the potential parameters, which will be a subject of our future work.

As examples, **Fig. 1** shows the calculated differential cross sections of elastically scattered 65 MeV protons for medium and heavy nuclides, such as ^{56}Fe, ^{100}Mo, ^{152}Sm, ^{184}W, and ^{232}Th. The computations were carried out by SRM-CC with the obtained Hamiltonian parameters described later. The calculated results reproduce not only the experimental data of 65 MeV protons[14–18] but also the measurements over a wide energy range below 200 MeV.

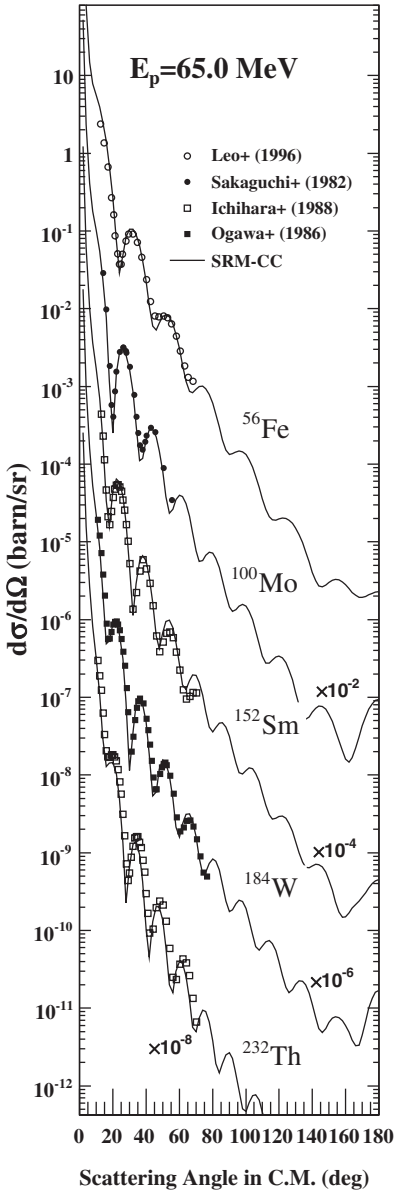

Fig. 1 Calculated elastic scattering differential cross sections of 65 MeV protons, which are compared with the experimental data[14–18] for ^{56}Fe, ^{100}Mo, ^{152}Sm, ^{184}W, and ^{232}Th. The computations were carried out by SRM-CC with the deduced Hamiltonian parameters.

(3) Coupled Levels

We just coupled major levels of $\tau = 1$ in the present analyses. These levels corresponded to the members of the G.S. and octupole bands, which were assigned as $\tau = 1$, $n_\gamma = 0$, $n_{\beta_2} = 0$, and $n_{\beta_3} = 0$. They were sufficient for obtaining the value of the deformation parameter β_{20} (and β_4 for typical deformed nuclei) uniquely from scattering data. The weakly coupled levels, *i.e.*, the γ- and β_2-vibrational states were purposely excluded from the CC calculations due to the reasons mentioned later.

The first 2^+ state is known to show the strongest collectivity among the low-lying levels in general. The succeeding $4_1^+, 6_1^+, \cdots$ levels are also relatively strong if the nucleus exhibits the rotational-vibrational or rotational property. Accordingly, we always included 0_1^+ and 2_1^+ for SRM-CC computation. Although we did not provide clear criteria for the inclusion of the additional levels $4_1^+, 6_1^+, \cdots$, the value of $E(4_1^+)/E(2_1^+)$ was a useful guide for this judgment. For examples, the levels $0_1^+, 2_1^+, (4_1^+)$ were coupled for the vibrational nuclides exhibiting $E(4_1^+)/E(2_1^+) \sim 2.0$. Meanwhile, the levels 0_1^+, 2_1^+, 4_1^+, 6_1^+, (8_1^+ and 10_1^+) were employed for the rotational-vibrational and rotational isotopes exhibiting $E(4_1^+)/E(2_1^+) \sim 3.0$. We always coupled the member of the octupole band 3_1^- together with the levels of the G.S. band. The coupling of this level did not affect significantly the calculated particle scattering cross sections from the 2_1^+ and 4_1^+ states, thereby, the values of β_{20} and β_4 to be determined, though the 3_1^- level tended to show a relatively strong collectivity for the vibrational and rotational-vibrational nuclei in general. However, since the measured inelastic scattering cross sections from the 3_1^- state were available for many nuclides, we included this level in order to investigate the validity of the octupole SRM parameters in terms of the cross sections.

The γ-vibrational states were not considered in the CC calculations because we could not determine the softness parameter value of γ-vibration, as mentioned in the previous section. Also, the β_2-vibrational states were not employed in our coupling scheme since SRM-CC sometimes inaccurately predicts the magnitude and/or angular distribution from the available experimental cross section data of 0_2^+. We consider that this could be due to the assumed band structures and/or imperfection of the model itself, which resulted in an insufficient description of the β_2-vibrational properties. However, it should be noted that such states are sufficiently weak to be negligible compared with the 2_1^+ and 3_1^- states.

3. Parameter Search

Since many SRM parameters must be determined simultaneously for each nucleus from limited experimental data, their values were deduced by a combination of automatic and manual searches to give the overall description of experimental level and inelastic scattering proton data. The search methods were based on our empirical insights, which were mostly devoted to giving an initial Hamiltonian parameter set. For example in the level structure analysis, we just assumed the quadrupole properties in the model as a first step. Then, a tentative quadrupole parameter set was estimated. Next, temporary octupole parameters were searched for. In this step, both quadrupole and octupole properties were considered by fixing the quadrupole parameter values. For typical deformed nuclei, the tentative hexadecapole parameters were also determined additionally. Thirdly, the quadrupole and octupole (and hexadecapole) parameters were determined almost simultaneously using the values obtained in the preceding two steps as the initial guesses. The final results were obtained by more than 20 iterations of the computer exercise for the three processes. The SRM-CC results sometimes could not reproduce the experimental angular distribution of (p, p') from 2_1^+ (and 4_1^+) around a backward angle. In such cases, we determined the values of the deformation parameters to describe the measured data in the forward region ($\theta_{\mathrm{C.M.}} \lesssim 40^\circ$), because the cross sections were not very sensitive to small differences in optical model potential in such an angular range.

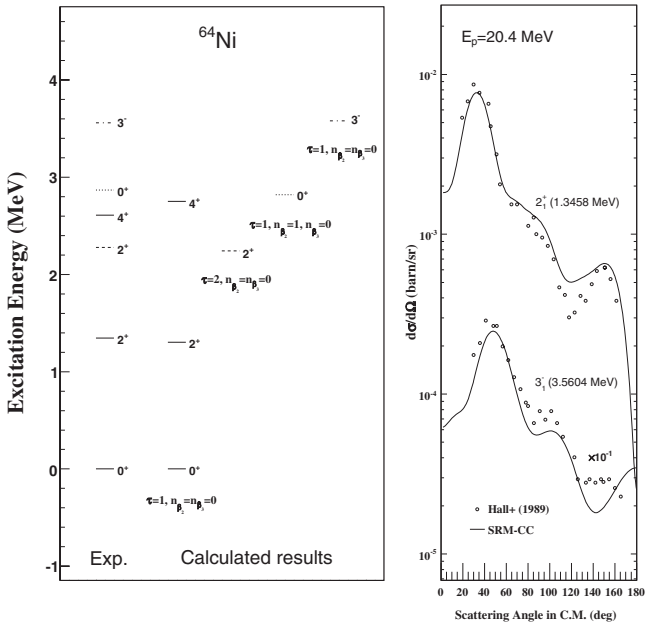

Fig. 2 SRM(-CC) calculations obtained with the present Hamiltonian parameters, which are compared with the experimental data for ^{64}Ni: the SRM low-lying level structure together with the experimental data (left) and the SRM-CC differential cross sections of inelastically scattered protons at 20.4 MeV together with measured data[19] (right)

Typical examples of the calculated and experimental levels are illustrated in **Figs. 2–4** together with those of (p, p') differential cross sections.[17–20] We could well describe the low-lying collective level structures of typical vibrational nuclei such as ^{64}Ni, rotational-vibrational nuclei such as ^{110}Pd, and rotational nuclei such as ^{232}Th. Also, SRM-CC reproduced the measured (p, p') differential cross sections from excitations of the 2_1^+ and 4_1^+ states only when we gave appropriate values of β_{20} and β_4. It should be noted that the measured 3_1^- cross sections are described fairly well. The worst result was obtained for ^{110}Pd, where the calculated result seems to disagree with the experimental data in phase by 10°. As for ^{232}Th and some other deformed nuclei, the present results reproduced the measured cross sections from excitations of 6_1^+. We should also mention that the obtained parameter values were almost consistent with those estimated in the past study[5] for ^{56}Fe.

III. Deduced Hamiltonian Parameters

1. Comparisons with the Experimental and Theoretical Results

The quadrupole deformation parameters were deduced by Raman *et al.*[21] from the measured electric-quadrupole transition probabilities $B(E2; 0_1^+ \rightarrow 2_1^+)$ for various even-even

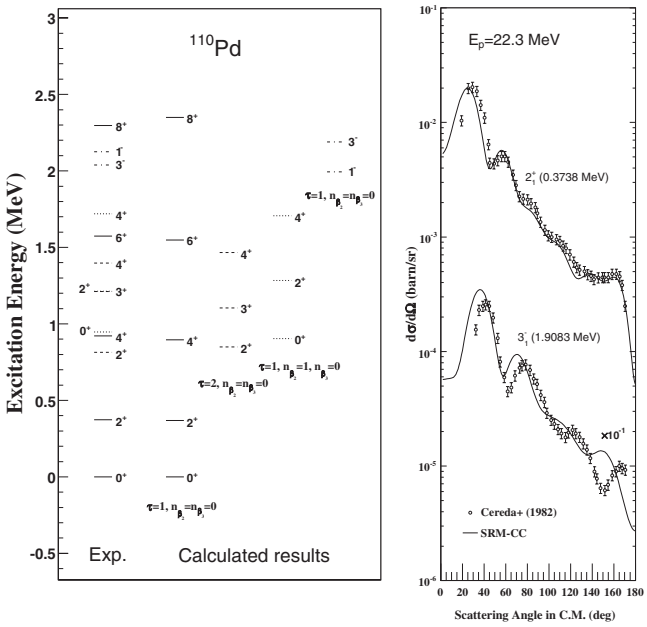

Fig. 3 SRM(-CC) calculations obtained with the present Hamiltonian parameters, which are compared with the experimental data for ^{110}Pd: the SRM low-lying level structure together with the experimental data (left) and the SRM-CC differential cross sections of inelastically scattered protons at 22.3 MeV together with measured data[20] (right)

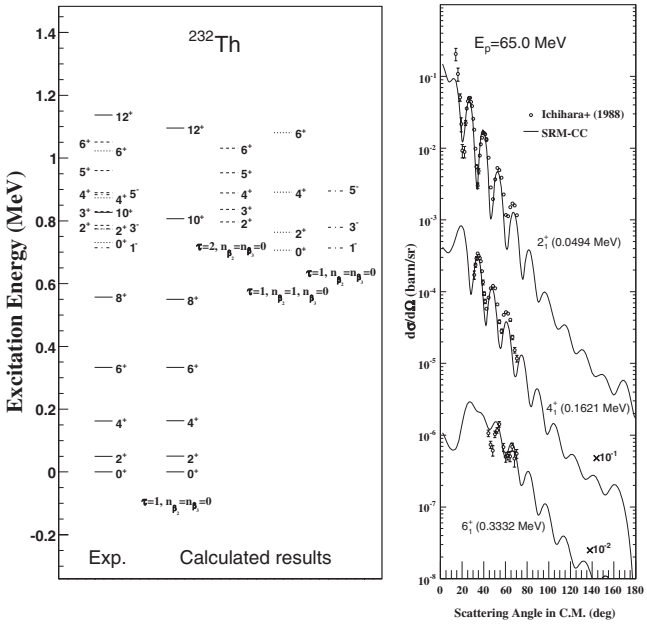

Fig. 4 SRM(-CC) calculations obtained with the present Hamiltonian parameters, which are compared with the experimental data for ^{232}Th: the SRM low-lying level structure together with the experimental data (left) and the SRM-CC differential cross sections of inelastically scattered protons at 65.0 MeV together with measured data[17,18] (right)

isotopes. Similarly, the octupole deformation was also extracted by Kibedi and Spear[22] from the measured electric-octupole transition probabilities $B(E3; 0_1^+ \rightarrow 3_1^-)$. Note that the obtained values correspond to the "effective" deformations that are attributed to both the rotation and the vibration. Thus, we used our effective deformations $\langle 0_1^+|\beta_2|2_1^+\rangle$ and $\langle 0_1^+|\beta_3|3_1^-\rangle$ for comparison with the experimental results obtained from $B(E2)$ and $B(E3)$ data. The results are shown in **Figs. 5** and **6**. Our quadrupole and octupole effective deformations reproduce the experimental data very well in both quantitative and qualitative senses aside from some exceptions. Discrepancies can be seen for typically deformed heavy nuclei, such as ^{150}Nd, ^{152,154}Sm, ^{160}Gd, ^{164}Dy, ^{166,168}Er, and ^{174,176}Yb, where the SRM-CC results underestimate the measured values by ∼20%. It is difficult to solve this problem at this stage. However, it should be

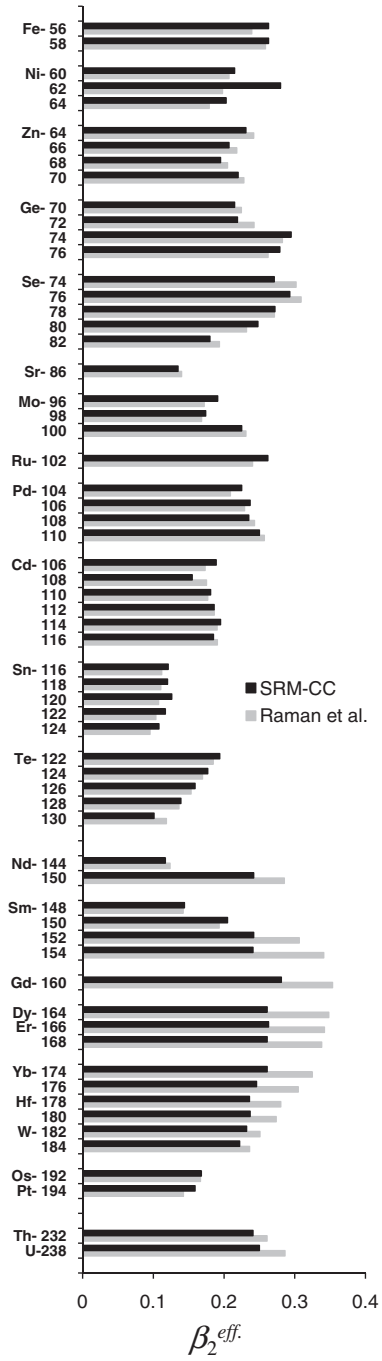

Fig. 5 The effective quadrupole deformation parameter is compared with the experimental data compiled by Raman *et al.*[21]

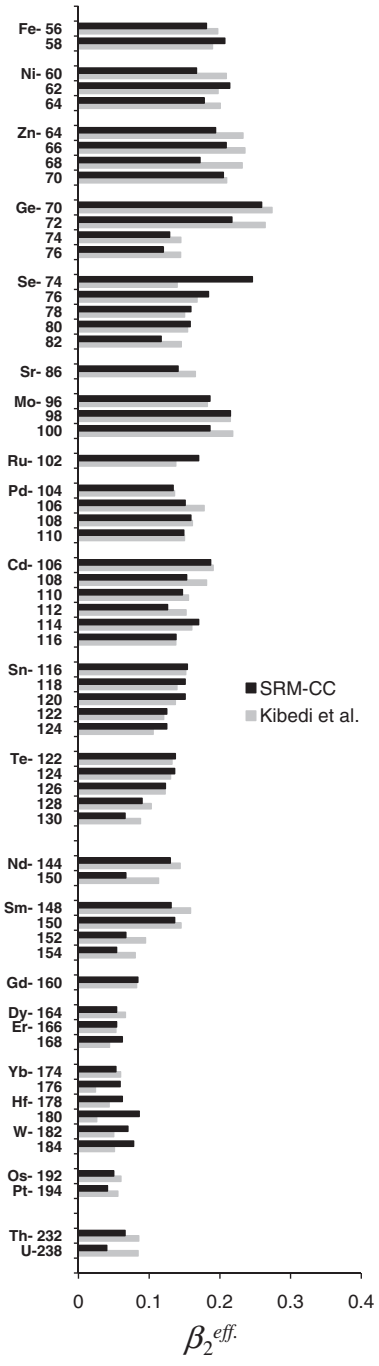

Fig. 6 The effective octupole deformation parameter is compared with the experimental data compiled by Kibedi and Spear[22)]

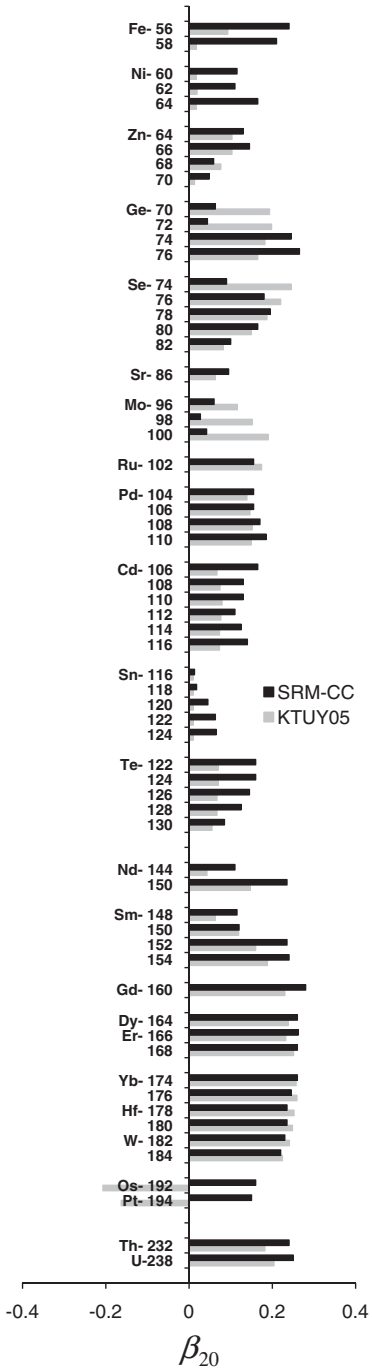

Fig. 7 The equilibrium quadrupole deformation parameter is compared with the theoretical values calculated by Koura *et al.*[25)]

noted that the deduced equilibrium G.S. deformation parameters (β_{20} and β_4) are almost consistent with the values obtained by the original CC analyses conducted by, *e.g.*, Ichihara *et al.*[17)] who employed simple but suitable models for such nuclei.

Some mass models have predicted systematically static deformations, which correspond to our equilibrium deformations. Our results should be compared with previously obtained values in order to determine the validity of present analyses. For theoretical deformations, we selected the finite range droplet model (FRDM),[23)] a Hartree-Fock-Bogoliubov (HFB) method based on the BSk2 Skyrme force,[24)] and the Koura-Tachibana-Uno-Yamada (KTUY) model.[25)] A comparison with the KTUY result is given in **Fig. 7** as an example. Our equilibrium G.S. quadrupole deformations also describe the gross tendency of the KTUY model predictions, though there are some exceptional isotopes or isotope regions for lighter nuclei. There is a fact that they become similar in the deformed heavy region ($A \gtrsim 150$). Similar trends are seen in the comparisons with the HFB and FRDM predictions. One can also see that the mass-model results sometimes have $\pm$ signs, which stand for symbolical nuclear shapes, *i.e.*, prolate (+) and oblate (−). However, the sign disagrees among theories very often. Therefore, the problem

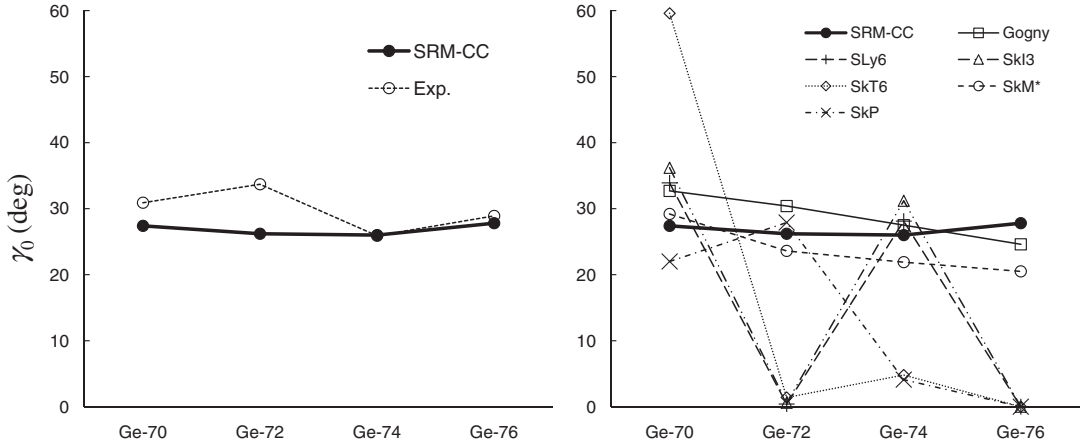

Fig. 8 γ_0 parameters of Ge isotopes compared with measured[26] (left panel) and theoretical[27] (right panel) data

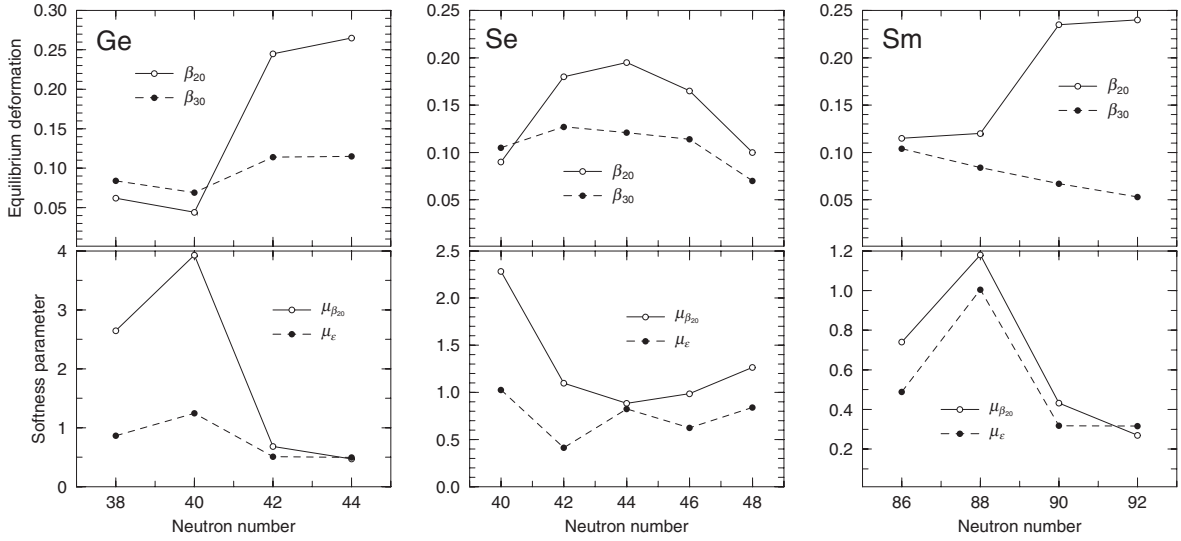

Fig. 9 Equilibrium quadrupole and octupole deformation parameters (upper panels) and corresponding softness parameters (bottom panels) for Ge (leftmost panels), Se (middle panels), and Sm (rightmost panels) isotopes

is not solved yet. In SRM, nuclear shape is determined on the basis of the γ_0 parameter, but we just plotted the β_{20} here.

Present results of β_{30} and β_4 usually deviate from the mass-model results. We do not discuss them because it is difficult to determine these small values quantitatively using the mass models in general.

Figure 8 shows a comparison of the presently deduced γ_0 parameters for Ge isotopes with experimental data[26] and theoretical results based on Gogny-Hartree-Fock-Bogoliubov and Skyrme Hartree-Fock-BCS models.[27] Our results are in very good agreement with the measured data. Although some disagreements are seen among the theoretical results, the predicted values with the Gogny and SkM* force parameter sets support our results.

2. Parameters in the Transitional Nuclei

The β_{20}, β_{30}, $\mu_{\beta_{20}}$, and μ_ϵ parameters of Ge, Se, and Sm isotopes are shown in **Fig. 9**. The deformation parameters of the Ge and Se isotopes clearly show the effect of the subshell at $N = 40$. The deformation parameters (both the quadrupole and octupole) of the $N = 38$ and 40 isotopes of Ge are less than 0.1, while those of the $N = 42$ and 44 isotopes are drastically larger. The occupation of the strongly deformed $\nu g_{9/2}$ orbit for isotopes above $N = 40$ is expected to produce such a drastic phenomenon. The same would occur for Se isotopes, while the large deformation is suppressed by $N = 50$ shell closure. The μ parameters of these isotopes are clearly anticorrelated with the deformation parameters. As was explained above, μ parameters express the softness of the longitudinal vibration. Therefore, those with a small equilibrium deformation are characterized by a strong vibrational excitation, while those with a large deformation are characterized by a stronger rotational excitation.

The situation is somewhat different for Sm isotopes. A similar jump of the quadrupole deformation parameter and an anticorrelated behavior in the μ parameters are present between $N = 88$ (^{150}Sm) and 90 (^{152}Sm), where no major shell exists. Such a change is consistent with a well-known shape transition corresponding to a U(5)-to-SU(3) transition in IBM and is probably attributable to the filling of the $\nu f_{7/2}$ orbit. On the contrary, the β_{30} parameter decreases monotonically.

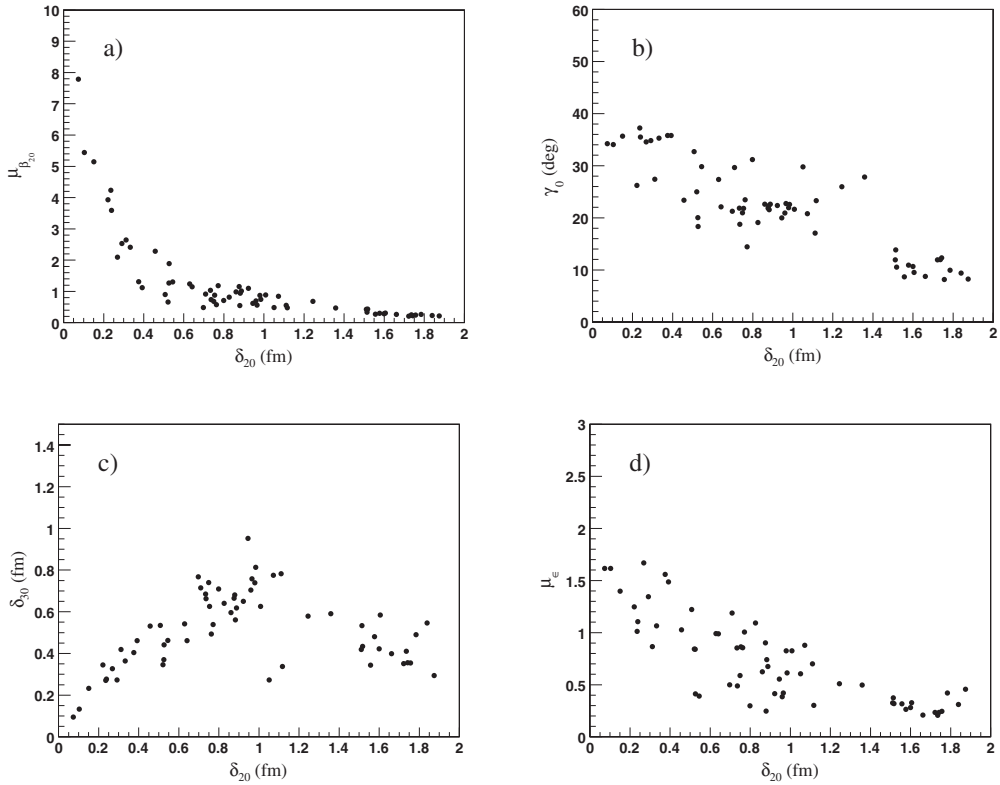

Fig. 10 Variations in major SRM Hamiltonian parameters as a function of quadrupole deformation length $\delta_{20}(= 1.21A^{1/3}\beta_{20})$ obtained in the present study: a) quadrupole softness parameter $\mu_{\beta_{20}}$, b) quadrupole nonaxial deformation parameter γ_0, c) octupole deformation length $\delta_{30}(= 1.21A^{1/3}\beta_{30})$, and d) octupole softness parameter μ_ϵ

3. Systematic Trends

According to our investigations, systematic trends can be seen among the major Hamiltonian parameters, such as β_{20}, $\mu_{\beta_{20}}$, γ_0, β_{30}, and μ_ϵ, as shown in **Figs. 10**(a)–10(d). Here, the equilibrium G.S. deformation was represented as the deformation length $\delta_{l0} = 1.21A^{1/3}\beta_{l0}\,\mathrm{fm}$ $(l = 2, 3)$ in order to express it as its absolute value. Although the obtained results show some visible fluctuations, the existence of regular behaviors indicates the possibility that we can predict the collective natures and/or low-lying level structures of many even-even nuclei by this phenomenological model analysis. The following items are devoted to the present features of each trend.

- Figure 10(a) shows the deduced $\mu_{\beta_{20}}$ values as a function of the δ_{20} values for all nuclides investigated in this analysis. We can see an apparent systematic trend between the parameters where it is expected to present a transitional behavior of the rotational-vibrational motion. The parameter $\mu_{\beta_{20}}$ increases at around $\delta_{20} \lesssim 0.2\,\mathrm{fm}$ and appears to reach an infinite value at $\delta_{20} = 0\,\mathrm{fm}$. This behavior is consistent with a fact that the spherical nucleus exhibits very typical vibrational properties. In practice, however, the applicability limit of the SRM might be around there. On the other hand, the values of $\mu_{\beta_{20}}$ decrease as those of δ_{20} increase, and they seem to gradually come close to zero. This means that the deformed heavy nuclei have an ellipsoidal surface where the β_2-vibrational properties are not so important (strong) at least for the low-lying states.
- Figure 10(b) presents the obtained values of γ_0 as a function of δ_{20}. A somewhat rough tendency is observed; however, the values surely decrease as δ_{20} parameters increase. The spherical nuclei are apt to exhibit $\gamma_0 \sim 30^\circ$, while the values of deformed heavy nuclei result in $\sim 10^\circ$. The quadrupole nonaxiality seems to be related with the shell structure of neutrons and/or protons. This probable behavior can be seen as a systematic trend in this figure. In the next paragraph, we would examine the point more closely and obtained findings are presented.
- Figure 10(c) shows the estimated values of δ_{30} as a function of δ_{20}. First, the values increase with δ_{20}. They take a maximum at $\delta_{20} \sim 1.0\,\mathrm{fm}$ and then gradually decline as the value of δ_{20} increase. Also, the values of these two parameters tend to be almost same up to $\sim 1.0\,\mathrm{fm}$. The phenomenon indicates that the large octupole equilibrium deformation is difficult to be formed.
- Figure 10(d) shows the results for the octupole softness constant μ_ϵ as a function of δ_{20}. Any clear systematic tendencies are not seen. This might be due to the low predictive power of the model and/or insufficient experimental information. However, the values surely decrease as δ_{20} increases, which is similar to the trend of $\mu_{\beta_{20}}$. The values of μ_ϵ do not exhibit a divergent behavior at $\delta_{20} \sim 0\,\mathrm{fm}$ unlike the trend of $\mu_{\beta_{20}}$. This implies that the closed and spherical shells are not extremely involved with the octupole vibrational property.

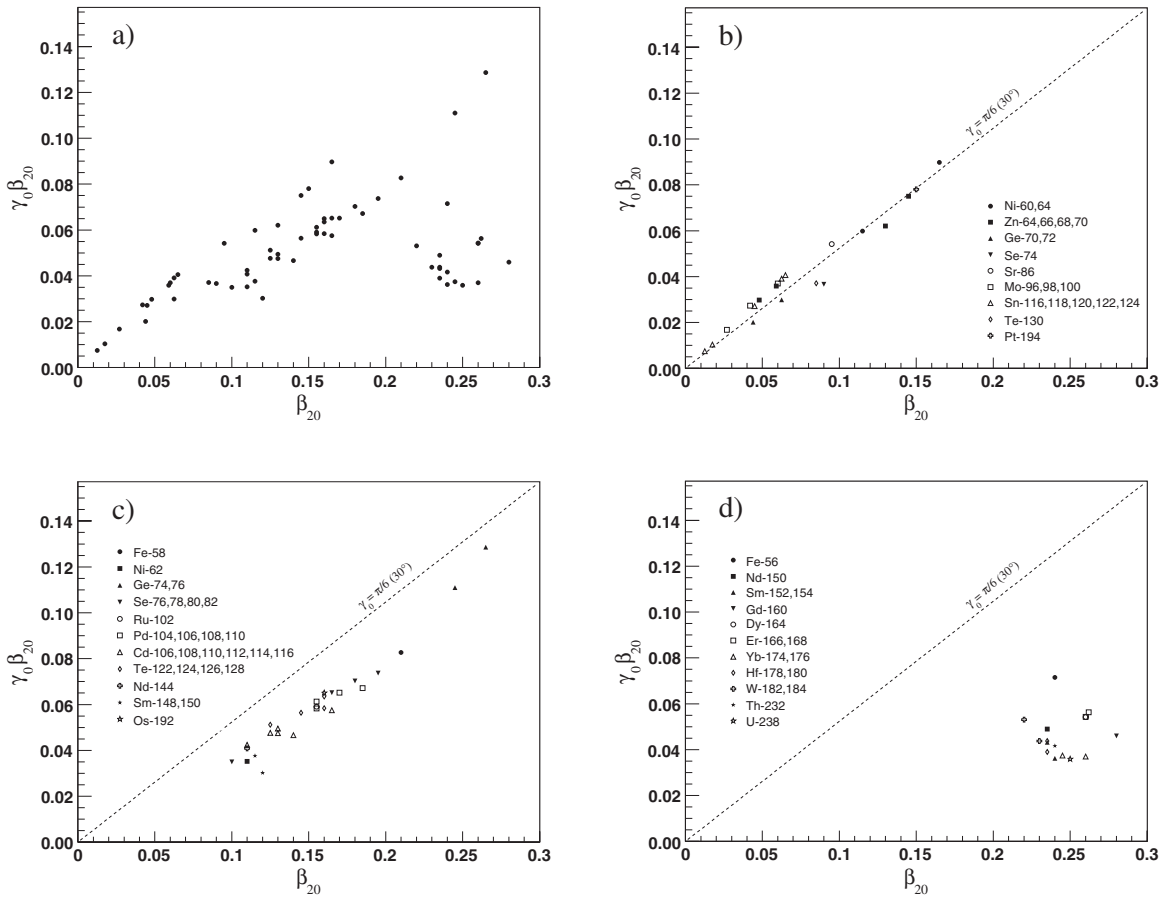

Fig. 11 Illustrations of the obtained values of $\gamma_0\beta_{20}$ as a function of β_{20}: a) for all nuclides, b) for nuclides whose γ_0-values are positioned around $\pi/6$ (30°), c) for nuclides whose γ_0-values slightly deviate from $\pi/6$, and d) for nuclides whose γ_0-values are away from $\pi/6$

The value of $\gamma_0\beta_{20}$ (or $\gamma_0\delta_{20}$) is a more suitable measure for investigating the nonaxial properties, since the quantity should express the absolute value of the equilibrium quadrupole asymmetric deformation. In **Fig. 11**(a), the obtained $\gamma_0\beta_{20}$ values are plotted as a function of the quadrupole static deformation β_{20} for all nuclei studied in this work. We can see that all data are positioned over a broad area, but they do not exceed the $\gamma_0 \sim \pi/6$ (30°) line. Moreover, it seems that the $\gamma_0 \sim \pi/6$ line behaves similarly to the limit of the quadrupole nonaxial parameter. In spite of this, however, there exist many nuclei that exhibit an almost middle shape ($\gamma_0 \sim \pi/6$) over a wide β_{20} range. These isotopes correspond to ^{60,64}Ni, $^{64–70}$Zn, ^{70,72}Ge, ^{74}Se, ^{86}Sr, ^{96,98,100}Mo, $^{116–124}$Sn, ^{130}Te, and ^{194}Pt. Their values are replotted in Fig. 11(b). It should be noted that these nuclei have a closed (sub-)shell core of neutrons or protons. We can also find another group that is positioned slightly below the $\gamma_0 = \pi/6$ line, as illustrated exclusively in Fig. 11(c). This includes the isotopes ^{58}Fe, ^{62}Ni, ^{74,76}Ge, $^{76–82}$Se, ^{102}Ru, $^{104–110}$Pd, $^{106–116}$Cd, $^{122–128}$Te, ^{144}Nd, ^{148,150}Sm, and ^{192}Os. Their neutron and/or proton numbers slightly deviate from the magic numbers. The remaining data are plotted in Fig. 11(d). It is difficult to identify a clear trend in this case due to the lack of data and the complicated shell structures.

Figure 12 presents the values of the quadrupole mass parameters, which are calculated with the estimated parameters (quadrupole mass parameter can be obtained using $B_2 = \frac{\hbar^2}{\hbar\omega_0 \cdot \mu^2_{\beta_{20}} \cdot \beta^2_{20}}$, where $\hbar\omega_0$ stands for the energy scale parameter in SRM). The data of ^{12}C and ^{28,30}Si are taken from Refs. 1) and 7), and they are plotted in this figure. As a global trend, the parameter increases with mass number, while such a behavior was not seen in the octupole and hexadecapole mass parameters. The visible local fluctuations are ascribed to the overall scale parameter $\hbar\omega_0$ as well as $\mu_{\beta_{20}}$ and β_{20}.

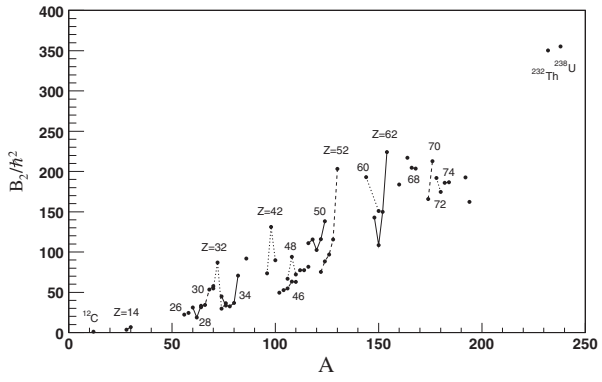

Fig. 12 Quadrupole mass parameters obtained in the present analyses as a function of the mass number A

IV. Conclusions

SRM-CC analyses were carried out for 63 even-even medium-heavy nuclei in order to see their individual collective behaviors and systematic trends. A complete SRM Hamiltonian parameter set was obtained for each nucleus by a combination of level structure and CC analysis for inelastically scattered protons. The deduced parameter values were expected to provide us with realistic and quantitative information on the equilibrium nuclear shape and rotational-vibrational characteristics. It was found that the values of major parameters, such as the softness and the equilibrium deformations, indicated the characteristics of each nucleus, which were mostly ascribed to the shell structure effects. The obtained values of the effective quadrupole and octupole deformations were found to be very close to the experimental data. In addition, equilibrium quadrupole deformation parameters were also found to exhibit a reasonable agreement with the mass-model results for deformed heavy nuclei. We can expect that the SRM-CC analysis is a useful approach to representing collective behaviors of a nucleus. Systematic trends were also seen among major Hamiltonian parameters. As well as the model itself, the findings are expected to give us a useful guide for elaborate nuclear data calculation.

A thorough description of the analysis procedure and a complete list of the deduced SRM Hamiltonian parameters will be given in a forthcoming report.[9)]

Acknowledgements

The authors would like to thank Drs. Yutaka Utsuno and Yosuke Toh of Japan Atomic Energy Agency (JAEA) for useful comments on the present work. They are also grateful to Dr. Jun-ichi Katakura of JAEA who promoted this study. This work was partly supported by a Grant-in-Aid for Scientific Research (C) 18560805 of Japan Society for the Promotion of Science.

References

1) S. Chiba, O. Iwamoto, Y. Yamanouchi *et al.*, "Consistent description of collective level structure and neutron interaction data for ^{12}C in the framework of the soft-rotator model," *Nucl. Phys.*, **A624**, 305 (1997).
2) E. Sh. Soukhovitskiĭ, S. Chiba, O. Iwamoto *et al.*, *Programs OPTMAN and SHEMMAN Version 8 (2004)*, JAERI-Data/Code 2005-002 (2005).
3) S. Chiba, O. Iwamoto, E. Sh. Sukhovitskiĭ *et al.*, "Coupled-channels optical potential for interaction of nucleons with ^{12}C up to 150 MeV in the soft-rotator model," *J. Nucl. Sci. Technol.*, **37**, 498 (2000).
4) E. Sh. Sukhovitskiĭ, Y.-O. Lee, J. Chang *et al.*, "Nucleon interaction with ^{58}Ni up to 150 MeV studied in the coupled-channels approach based on the soft-rotator nuclear structure model," *Phys. Rev.*, **C62**, 044605 (2000).
5) E. Sh. Sukhovitskiĭ, S. Chiba, J.-Y. Lee *et al.*, "Nuclear level structure, B(E2) gamma-transitions and nucleon interaction data for ^{56}Fe by a unified soft-rotator model and couple-channels framework," *J. Nucl. Sci. Technol.*, **39**, 816 (2002).
6) E. Sh. Sukhovitskiĭ, S. Chiba, J.-Y. Lee *et al.*, "Analysis of nucleon scattering data of ^{52}Cr with a coupling scheme built with the soft-rotator model," *J. Nucl. Sci. Technol.*, **40**, 69 (2003).
7) W. Sun, Y. Watanabe, E. Sh. Sukhovitskiĭ *et al.*, "Coupled-channels analysis of nucleon interaction data of ^{28,30}Si up to 200 MeV based on the soft rotator model," *J. Nucl. Sci. Technol.*, **40**, 635 (2003).
8) S. Kunieda, S. Chiba, K. Shibata *et al.*, "Systematical nucleon-induced optical model analysis for medium and heavy nuclei with coupled-channel framework," *Proc. Int. Conf. Nuclear Data for Science and Technology*, Nice, France, Apr. 22–27, 2007, EDP Sciences, 227–230 (2008).
9) S. Kunieda, S. Chiba, K. Shibata *et al.*, to be submitted as JAEA report.
10) A. S. Davydov, A. A. Chaban, "Rotation-vibration interaction in non-axial even nuclei," *Nucl. Phys.*, **20**, 499 (1960).
11) Yu. V. Porodzinskiĭ, E. Sh. Sukhovitskiĭ, "Incorporating hard hexadecapole modes in a phenomenological collective nuclear model with five dynamical variables," *Yad. Fiz.*, **55**, 2368 (1992).
12) Yu. V. Porodzinskiĭ, E. Sh. Sukhovitskiĭ, "Analysis of neutron scattering by even-even nuclei with allowance for dynamical octupole deformations," *Yad. Fiz.*, **59**[2], 247 (1996).
13) S. Kunieda, S. Chiba, K. Shibata *et al.*, "Coupled-channels optical model analyses of nucleon-induced reactions for medium and heavy nuclei in the energy region from 1 keV to 200 MeV," *J. Nucl. Sci. Technol.*, **44**, 838 (2007).
14) R. De Leo, H. Akimune, N. Blasi *et al.*, "Isospin character of low-lying states in ^{56}Fe," *Phys. Rev.*, **C53**, 2718 (1996).
15) H. Sakaguchi, M. Nakamura, K. Hatanaka *et al.*, "Elastic scattering of 65 MeV polarized protons," *Phys. Rev.*, **C26**, 944 (1982).
16) H. Ogawa, H. Sakaguchi, M. Nakamura *et al.*, "Inelastic scattering of 65-MeV polarized protons from ^{178}Hf, ^{180}Hf, ^{182}W, and ^{184}W and multipole moments of the optical potential," *Phys. Rev.*, **C33**, 834 (1986).
17) T. Ichihara, H. Sakaguchi, M. Nakamura *et al.*, "Inelastic proton scattering exciting the γ-vibrational band in deformed nuclei ($152 \leq A \leq 192$) at 65 MeV and the systematics of the hexadecapole (Y_{42}) strength of the γ-vibration," *Phys. Rev.*, **C36**, 1754 (1987).
18) T. Ichihara, "Systematics of the hexadecapole (Y_{42}) strength of the γ-vibration in deformed nuclei ($152 \leq A \leq 192$) from inelastic scattering of polarized protons at 65 MeV," *Mem. Fac. Sci., Kyoto Univ., Ser. Phys. Astrophys., Geophys. Chem.*, **C37**, 191 (1988).
19) P. J. van Hall, S. D. Wassenaar, S. S. Klein *et al.*, "Scattering of polarized protons by Ni, Sr, Cd, In and Sn isotopes: II. Inelastic scattering—collective analysis," *J. Phys.*, **G15**, 199 (1989).
20) E. Cereda, M. Pignanelli, S. Micheletti *et al.*, "Proton scattering on $A = 92$–116 nuclei with extended optical models and the interacting boson approximation," *Phys. Rev.*, **C26**, 1941 (1982).
21) S. Raman, C. W. Nestor, P. Tikkanen, "Transition probability from the ground to the first-excited 2^+ state of even-even nuclides," *At. Data Nucl. Data Tables*, **78**, 1 (2001).
22) T. Kibedi, R. H. Spear, "Reduced electric-octupole transition probabilities, $B(E_3; 0_1^+ \rightarrow 3_1^-)$—An update," *At. Data Nucl. Data Tables*, **80**, 35 (2002).
23) P. Moller, J. R. Nix, W. D. Myers *et al.*, "Nuclear ground-state masses and deformations," *At. Data Nucl. Data Tables*, **59**, 185 (1995).

24) S. Goriely, M. Samyn, P. H. Heenen *et al.*, "Hartree-fock mass formulas and extrapolation to new mass data," *Phys. Rev.*, **C66**, 024326 (2002).
25) H. Koura, T. Tachibana, M. Uno *et al.*, "Nuclidic mass formula on a spherical basis with an improved even-odd term," *Prog. Theor. Phys.*, **113**, 305 (2005).
26) Y. Toh, T. Czosnyka, M. Oshima *et al.*, "Coulomb excitation of ^{74}Ge beam," *Eur. Phys. J.*, **A9**, 353 (2000).
27) L. Guo, J. A. Maruhn, P.-G. Reinhard, "Triaxiality and shape coexistence in germanium isotopes," *Phys. Rev.*, **C76**, 034317 (2007).